

## Accepted Manuscript

$\delta^{13}\text{C}_{org}$  and *n*-alkane evidence for changing wetland conditions during a stable mid-late Holocene climate in the central Tibetan Plateau

Man-Ching Cheung, Yongqiang Zong, Ning Wang, Jonathan C. Aitchison, Zhuo Zheng

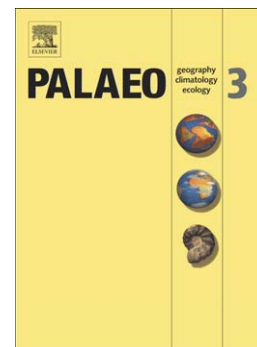
PII: S0031-0182(15)00434-4  
DOI: doi: [10.1016/j.palaeo.2015.08.007](https://doi.org/10.1016/j.palaeo.2015.08.007)  
Reference: PALAEO 7406

To appear in: *Palaeogeography, Palaeoclimatology, Palaeoecology*

Received date: 15 January 2015  
Revised date: 7 August 2015  
Accepted date: 8 August 2015

Please cite this article as: Cheung, Man-Ching, Zong, Yongqiang, Wang, Ning, Aitchison, Jonathan C., Zheng, Zhuo,  $\delta^{13}\text{C}_{org}$  and *n*-alkane evidence for changing wetland conditions during a stable mid-late Holocene climate in the central Tibetan Plateau, *Palaeogeography, Palaeoclimatology, Palaeoecology* (2015), doi: [10.1016/j.palaeo.2015.08.007](https://doi.org/10.1016/j.palaeo.2015.08.007)

This is a PDF file of an unedited manuscript that has been accepted for publication. As a service to our customers we are providing this early version of the manuscript. The manuscript will undergo copyediting, typesetting, and review of the resulting proof before it is published in its final form. Please note that during the production process errors may be discovered which could affect the content, and all legal disclaimers that apply to the journal pertain.



$\delta^{13}\text{C}_{\text{org}}$  and *n*-alkane evidence for changing wetland conditions during a stable mid-late

### Holocene climate in the central Tibetan Plateau

Man-Ching Cheung <sup>a</sup>, Yongqiang Zong <sup>a,\*</sup>, Ning Wang <sup>b</sup>, Jonathan C. Aitchison <sup>c</sup>, Zhuo Zheng <sup>d</sup>

<sup>a</sup> *Department of Earth Sciences, the University of Hong Kong, Hong Kong SAR, China*

<sup>b</sup> *Guangzhou Institute of Geochemistry, Chinese Academy of Science, Guangzhou, China*

<sup>c</sup> *School of Geography Planning and Environmental Management, The University of Queensland, Brisbane, Queensland, Australia*

<sup>d</sup> *Department of Earth Sciences, Sun Yat-Sen University, Guangzhou, China*

Corresponding author at: University of Hong Kong, Hong Kong SAR, China

Tel: +852 39174815. *E-mail address:* yqzong@hku.hk (Y. Zong)

### ABSTRACT

This study has examined bulk and compound specific organic carbon isotopes ( $\delta^{13}\text{C}_{\text{org}}$ ) and lipid *n*-alkanes of modern plants and a wetland sediment sequence from the central Tibetan Plateau and explores the usefulness of these two methods for palaeoenvironmental reconstructions. Results show that a combination of  $\delta^{13}\text{C}_{\text{org}}$  values and *n*-alkane indices can help differentiate organic matter from C3 terrestrial plant, C4 terrestrial plant and submerged

macrophytes, the three main sources of organic matter in the study area. The analyses of total organic carbon,  $\delta^{13}\text{C}_{\text{org}}$  values and *n*-alkane indices for the sediment sequence imply that a wetland habitat was established about 8000 years ago, and the wetland conditions were largely stable with dominantly C3 wetland herbs covering the wetland. However, small fluctuations in the dominant organic matter supply between vascular and aquatic plants are revealed, suggesting short duration changes in the extent of open water area within the wetland or variations in the productivity of submerged macrophytes and aquatic plants within the wetland ecosystem, which reflects variations in the strength of precipitation and evaporation.

**Keywords:**

Organic carbon isotopes, *n*-alkane indices, alpine wetland, monsoon climate change, Tibetan Plateau

**1. Introduction**

Organic carbon geochemical methods have been widely applied for palaeoenvironmental studies from lake sediments (e.g. Meyers and Ishiwatari, 1993; Meyers et al, 1994; Lamb et al, 2004). Earlier studies tend to use the total organic matter (TOC), ratios of total carbon to total nitrogen (C/N), and later organic carbon isotopes ( $\delta^{13}\text{C}_{\text{org}}$ ), that are preserved in sediments as indicators for the identification of organic carbon sources and

thus vegetation changes associated with palaeoclimatic histories (Kohn, 2010; Wang et al., 2002). To reveal large scale climatic fluctuations such as glacial-interglacial changes, these methods have proven very useful because changes commonly involve alterations between dry and wet environmental conditions, and thus TOC can show high or low productivity of organic matter, C/N ratios can indicate changes between aquatic and non-aquatic environments, and  $\delta^{13}\text{C}_{\text{org}}$  can detect variations of C3 and C4 plant communities (Huang et al., 2001; Tieszen et al., 1979). However, when these methods are applied to studies of the generally stable Holocene period, further understanding of these methods is required. In particular, interpretations of organic geochemical data must be made according to regional context. Recently, organic biomarkers such as *n*-alkane distributions have also been added to the tool-box for palaeoenvironmental reconstructions (e.g. Aichner et al., 2010; Lin et al., 2008; Mügler et al., 2010; Wang et al., 2014). These new methods need to be tested in many different climatic regions. In this study, we collected plant samples from central Tibetan Plateau, analysed their  $\delta^{13}\text{C}$  ratios and *n*-alkane distributions, and then applied these organic geochemical techniques to a sediment core obtained from an alpine wetland of the study area and evaluated the methods in order to improve palaeoenvironmental reconstructions in high altitude regions.

## 2. Study site, materials and methods

The Tibetan Plateau with an average elevation above 4000 m covers an area of 1.22 million km<sup>2</sup> (Fig. 1a). Due to its high altitude and the massive extent of this plateau, it draws moisture northwards from the Indian Ocean during the summer. In the winter, the mid-latitude jet stream from the northwest has a strong influence on the plateau environment. The combination of the two atmospheric systems and the high mountain ranges on the plateau creates a high diversity amongst plant biomass and ecosystems across the region (Fig. 2). At present, alpine forest only occurs along river valleys and mountain slopes on the southern and eastern edges of the Plateau. For instance, Cupressaceae, *Populus*, *Salix* and other shrubs are common around 3600 m above sea level (a.s.l.) within the Yarlung Tsangpo valley. Such vegetation extends upstream to a little higher at 3840 m (a.s.l.) west of Shigatse, with *Salix* occurring as high up as 4330 m (a.s.l.) at Lhaze and 4310 m (a.s.l.) around Tingri. No trees are seen at altitudes >4500 m (a.s.l.) in these areas. Also within river valleys and around lakesides, such as Yamdrok Yum Cuo, 4500 m (a.s.l.), extensive marshes are found in which the wetland herbs Asteraceae, Cyperaceae, Poaceae, Leguminosae, Plantaginaceae and Ranunculaceae dominate. On the hill slopes, however, dry-land herbs such as *Artemisia*, Cyperaceae and Poaceae are sparsely distributed. In the northwestern half of the Plateau the dry-land herbs communities are increasingly dominated by Chenopodiaceae, together with *Artemisia*. Also in the northwestern half of the Plateau wetland communities can still be found along lakesides. For instance, at Zhari Nam Co and

Dawa Co (4700 m a.s.l), Cyperaceae and Poaceae are common along streams and lakesides.

Within some freshwater lakes, aquatic plants (*Potamogeton*, *Myriophyllum*, *Batrachium* and *Hippuris*) and submerged macrophytes (*Chara sp.*) are found (e.g. Aichner et al., 2010).

To understand the organic carbon signatures of organic matters, plant samples (leaves) including trees, shrubs and herbs have been collected from the central area of the Plateau (Fig. 1a). This sampling strategy was designed to test if organic geochemical signatures from these plants samples can reflect the environmental or climatic conditions where they live, prior to palaeoenvironmental reconstructions. In total, thirty-four terrestrial plant leaves including 7 trees, 4 shrubs, 19 herbs with C3 photosynthesis pathways and 4 herbs with C4 photosynthesis pathways were collected in this study (Table 1). Together with analyses of macrophytes by Aichner et al. (2010), these samples form a data set that fully represents the alpine vegetation of the study area.

A sediment core was obtained from a valley-floor wetland on the southeastern side of the Nyaningtanglha Mountain Range, about 10 km northeast of Dangxiong (Fig. 1b). It is an inter-montane valley fed by melt-water from ice-caps on the surrounding mountain peaks. According to the local weather station, the mean annual precipitation is 480 mm, and the mean annual temperature is 1.7 °C. Summer temperature (May to September) can be up to 9.2°C at present. In the field, a Russian-type hand drilling auger was used to extract a peat sequence (CN01) c. 100 m into the wetland. A small open water area was still present at the

centre of the wetland. The sediment sequence is 5.80 m long and undisturbed. It was wrapped in tin foil and stored at low temperature to keep the organic sediment from oxidation and contamination.

Fresh leaves from plant samples were selected and the sediment core was subsampled every 3 cm for analyses. All samples were freeze dried and grounded into powder. About 1 mg of each plant sample and 3 mg of each sediment sample were combusted within capsules in an Elemental Analyzer linked to an Isotope Ratio Mass Spectrometer (EA-IRMS), from which total organic carbon (TOC), total nitrogen (TN) and stable isotope ratios ( $\delta^{13}\text{C}_{\text{org}}$ ) of each sample were measured. The rest of the dry material from each sample was digested into soluble organic matter using organic solvent with HPLC grade dichloromethane (DCM) and methanol (MeOH) mixture by an ultrasonic extractor. The extraction processes were repeated three times, and the total lipid extracts were then dried and saponified with 6% KOH/MeOH to separate the acidic and neutral lipid fractions. This was followed by lipids being separated in a silica gel column chromatography eluting with *n*-hexane, DCM and MeOH to isolate different polar compositions in neutral fractions. Finally, the extracts were injected into a gas-chromatograph coupled with flame ionisation detection (GC-FID) for *n*-alkane identification. The lipid *n*-alkanes analysis in aliphatic fractions was performed in a GC. The GC oven programme was set as follows, rinsing from the initial temperature of 60 °C to 250 °C at a rate of 20 °C/min, then to 270 °C at a rate of 5 °C/min and finally to 310 °C at a

rate of 2 °C/min and holding isothermally for 15 minutes. A mixture of external standards of *n*-C21, *n*-C25, *n*-C27, *n*-C29, *n*-C31 and *n*-C33 was used to identify the *n*-alkanes peaks while *n*-C36 standard of a known concentration was used to quantify the *n*-alkanes compounds.

40 samples from different depths of the core were further analysed for the stable isotope ratios of organic compounds in a GC-IRMS. The GC was set on splitless injection and used helium as the carrier gas. The temperature was first held at 50 °C for 2 minutes, and increased to 200 °C at a rate of 20 °C /min, then to 300 °C at a rate of 3 °C /min and subsequently held isothermally for another 10 minutes. A standard mixture from *n*-C16 to *n*-C30 was employed for the identification of *n*-alkanes peaks for isotopic measurement in the IRMS. Results were expected to help differentiate organic sources between C4 plant matter and C3 aquatic organic matter.

In order to elucidate the relationship between *n*-alkane compounds and palaeoenvironmental conditions, the relative abundance of the most concentrated compound ( $C_{max}$ ) from each sample was identified from the GC outputs, with carbon preference index (CPI), average chain length (ACL) and proportion of aquatic plants *n*-alkane ( $P_{aq}$ ) calculated according to the equations below,

$$CPI = ((C_{23}+C_{25}+C_{27}+C_{29}+C_{31}) / (C_{24}+C_{26}+C_{28}+C_{30}+C_{32})) + \\ (C_{25}+C_{27}+C_{29}+C_{31}+C_{33}) / (C_{24}+C_{26}+C_{28}+C_{30}+C_{32})) / 2$$

(according to Allan and Douglas, 1977)



$$ACL_{23-31} = (C_{23} \times 23 + C_{25} \times 25 + C_{27} \times 27 + C_{29} \times 29 + C_{31} \times 31) / (C_{23} + C_{25} + C_{27} + C_{29} + C_{31})$$

(modified after Poynter, 1989 to include C<sub>23</sub> and C<sub>25</sub>)

$$P_{aq} = (C_{23} + C_{25}) / (C_{23} + C_{25} + C_{29} + C_{31})$$

(according to Ficken et al., 2000)

Seven samples of plant fragments were selected from different depths for radiocarbon dating analysis. Each date was calibrated to calendar years before present (1950 AD) with CALIB 5.10 (Stuiver et al., 1998).

### 3. Results and interpretation

#### 3.1. Plant samples

A total of 34 plant samples were analysed in this study. Details of their species, habitats and altitude information, organic carbon isotope ( $\delta^{13}C_{org}$ ) values and *n*-alkane indices are listed in Table 1, along with results of submerged macrophyte samples from the study area provided by Aichner et al. (2010). The data are arranged by species and grouped into tree, shrubs, C<sub>4</sub> herbs, C<sub>3</sub> herbs and submerged macrophytes for interpretation and discussion.

Bulk  $\delta^{13}C_{org}$  values for tree samples fall into a narrow range of  $-26.1 \pm 0.7$  ‰, and the values for shrubs are around  $-25.8 \pm 0.6$  ‰. Samples of herbs show two distinctive groups, with the values for C<sub>4</sub> herbs ranging narrowly between  $-13.3$  ‰ and  $-15.3$  ‰ ( $-13.9 \pm 0.9$  ‰), whilst the values for C<sub>3</sub> herbs vary from  $-25.0$  ‰ to  $-27.9$  ‰ ( $-26.4 \pm 0.9$  ‰). In other words,

there is very little difference in the  $\delta^{13}\text{C}_{\text{org}}$  values among samples of trees, shrubs and C3 herbs analysed in this study. These C3 plant specimens are from different altitudes between 3600 m and 6100 m, i.e. there is no relationship between plant  $\delta^{13}\text{C}_{\text{org}}$  values and their altitudes. Furthermore, there is no difference between C3 herbs from dry surface (hill slope, sand dune and raised terraces) and wet surface (lakeside and river/streamside). The four C4 herbs are of Cyperaceae, which appear sparsely as patches on the dryer mountain slope of middling altitudes (3800–4700 m). The bulk  $\delta^{13}\text{C}_{\text{org}}$  values for submerged macrophytes are similar to those of C4 herbs.

The carbon number with maximum *n*-alkanes concentration ( $C_{\text{max}}$ ) from the plant samples reveals an interesting pattern (Table 1). The  $C_{\text{max}}$  of trees varies greatly but centres at 27. The  $C_{\text{max}}$  of shrubs is concentrated at 29. For herbs in wetland or dryland habitats, the  $C_{\text{max}}$  is at either 29 or 31. Submerged macrophytes, however, have a much lower  $C_{\text{max}}$  of 23. The ACL index closely follows the  $C_{\text{max}}$ , i.e. variable  $\text{ACL}_{23-31}$  for trees, similar  $\text{ACL}_{23-31}$  for shrubs and herbs, and much lower  $\text{ACL}_{23-31}$  for submerged macrophytes. CPI for trees is mostly higher than 20, with C3 wetland herbs around 12 and C3 dryland herbs mostly lower than 10. CPIs for shrubs, C4 herbs and submerged macrophytes are all highly variable.  $P_{\text{aq}}$  seems to be a useful index for differentiating submerged macrophytes from herbaceous plants, as the majority of herbs has a  $<0.2 P_{\text{aq}}$  whilst the values for most submerged macrophytes are mostly  $>0.7$ . Nevertheless none of these indices show any correlation

with altitude.

Table 2 shows the average values of plant  $\delta^{13}\text{C}_{\text{org}}$  at major odd carbon chain lengths. As expected, the values for C4 herbs and submerged macrophytes are significantly enriched in all carbon chains at around -22‰ compared with those from trees, shrubs and C3 herbs generally between -30‰ and -33‰. Secondly, the variation among the  $\delta^{13}\text{C}_{\text{org}}$  values of different odd carbon chain lengths for trees, shrubs and C3 herbs is not as significant as those of C4 herbs and submerged macrophytes. Thirdly, the  $\delta^{13}\text{C}_{\text{org}}$  values for C4 herbs and submerged macrophytes are depleted progressively with longer carbon chains, and there is no progressive depletion with longer carbon chains for trees, shrubs and C3 herbs.

### **3.2. Core sediment**

The lithostratigraphy of the 5.8m-long core is presented in Table 3, and is composed of three sedimentary units. The basal unit (5.22–5.80 m) contains sandy silt and small pebbles, with little organic matter, as indicated by the close-to-zero TOC values (Fig. 3a, b). Towards the top end of this unit, organic matter increases as sandy material decreases. The middle unit (0.95–5.20 m) consists of almost pure organic matter, and its organic carbon content remains around 35% and becomes a little lower in 1.80–0.95 m. An increase in silt is noted in the top unit (0.28–0.95 m). The sedimentary chronology developed based on the 7 AMS radiocarbon dates from plant fragments (Table 4) suggests the sedimentation started at least c. 10,000 years ago. The calibrated ages yield a polynomial age-depth relationship for the

core. From the base of the core to about 6000 Cal. yrs BP covering the thin, basal gravelly sand layer and the transition into the middle sedimentary unit, a lower sedimentation rate (c. 0.27 mm/a) is observed. Between 6000 and 2000 Cal. yrs BP which include the bulk of the middle sedimentary unit, a higher sedimentation rate (c. 0.85 mm/a) was recorded. During the final 2000 years or in the top sedimentary unit, the sedimentation rate slowed down a little to c. 0.64 mm/a. On average, sub-samples at 3 cm intervals represent a roughly 50-year resolution for the core.

The bulk  $\delta^{13}\text{C}_{\text{org}}$  values from the sediment (Fig. 3c) fluctuate between -24.8‰ and -27.8‰. Together with the lithostratigraphy and TOC, the variations in bulk  $\delta^{13}\text{C}_{\text{org}}$  value of the core suggest eight stages of environmental change. Stages I, III, V and VII are associated with relative enrichment in bulk  $\delta^{13}\text{C}_{\text{org}}$ , whilst more depleted values are noted in Stages II, IV, VI and VIII. Compound specific  $\delta^{13}\text{C}_{\text{org}}$  values from these stages are summarized in Table 5, which shows no significant variation throughout the core.

The sediment samples from core CN01 contain *n*-alkanes from carbon chain lengths between *n*-C18 and *n*-C35, from which most samples express their maximum *n*-alkanes concentration at various carbon number ( $C_{\text{max}}$ ), ranging from *n*-C21 to *n*-C31 (Fig. 3d). The  $C_{\text{max}}$  from lower section of the core appears to be generally at *n*-C21, and it progressively increases from *n*-C25 to *n*-C31 towards the upper section of the core. In Stages IV and VIII, some samples have their  $C_{\text{max}}$  at *n*-C29 and *n*-C31. Variations of  $\text{ACL}_{23-31}$  and  $P_{\text{aq}}$  follow a

pattern similar to the bulk  $\delta^{13}\text{C}_{\text{org}}$  curve (Fig. 3c, e, f). Higher values of  $\text{ACL}_{23-31}$  appear in Stages IV, VI and VIII, corresponding to the more depleted bulk  $\delta^{13}\text{C}_{\text{org}}$  values. In these three stages, relatively lower  $P_{\text{aq}}$  values are also recorded. The pattern of CPI is slightly different, although variations of CPI values follow the general trend of bulk  $\delta^{13}\text{C}_{\text{org}}$  values between stages (Fig. 3g).

## 4. Discussion

### 4.1. $\delta^{13}\text{C}_{\text{org}}$ values and n-alkane indices from modern plants

Some previous researchers have proposed that, altitudinal change could affect the bulk  $\delta^{13}\text{C}_{\text{org}}$  values of vascular plants (Korner et al, 1988; Sparks and Ehleringer, 1997; Menot and Burns, 2001). Furthermore, some studies suggested that C4 herbs are distributed according to altitude (Menot and Burns, 2001; Stevenson et al, 2005; Wang, 2003) and geographic location (Korner, 1991; Wang et al, 2004). In our study the two most common species, Cyperaceae and Poaceae, occur between 3600 m and 6100 m across the central Tibetan Plateau (Table 1), and the result shows no altitudinal relationship with the  $\delta^{13}\text{C}_{\text{org}}$  values among both C3 and C4 herbs. The  $\delta^{13}\text{C}_{\text{org}}$  values of C3 and C4 herbs do not vary according to latitude and longitude either, despite C3 herbs dominating wetland vegetation in the east and southeast parts of the Plateau, whilst C4 herbs are more common in the west and northwest parts of the Plateau.

As Table 1 illustrates, modern plant samples fall into two distinctive groups. C4 herbs and submerged macrophytes have a  $\delta^{13}\text{C}_{\text{org}}$  value centered about -15.0‰. Trees, shrubs and C3 herbs have their  $\delta^{13}\text{C}_{\text{org}}$  values varying between -25.0‰ and -28.0‰. The difference between these two end members is significant, suggesting that  $\delta^{13}\text{C}_{\text{org}}$  signatures from plants can be used for differentiating these two sources of organic matter. For lake or wetland sediment, however,  $\delta^{13}\text{C}_{\text{org}}$  values alone are insufficient to help differentiating organic matter sources between C4 herbs and submerged macrophytes because they share a similar  $\delta^{13}\text{C}_{\text{org}}$  signature. To solve this problem, additional data are needed. In this study, we have found *n*-alkane indices useful.

*n*-alkanes exist widely in epicuticula waxes of plant with a function of maintaining water in leaves. Positive correlation is considered to exist between the melting point of a leaf wax and the highest leaf temperature (Eglinton and Hamilton, 1967; Sachse et al., 2006). Previous researchers suggest that *n*-alkane distributions of aquatic algae and bacteria generally maximize at *n*-C17 and distinctly differ from vascular plants which mainly contain *n*-alkanes of mid to long chains in *n*-C21-C31 (Cranwell, 1987; Rieley, 1991; Ficken, 2000). Within the group of vascular plants, submerged and floating macrophytes are believed to contain large proportions of *n*-C21, *n*-C23 and *n*-C25 alkanes (Aichner et al., 2010), whilst terrestrial plants have abundant *n*-C27, *n*-C29 and *n*-C31 alkanes (Cranwell, 1984; Ficken, 2000). In other words, *n*-alkanes can be an ideal addition to the  $\delta^{13}\text{C}_{\text{org}}$  ratios for differentiating organic

matter sources between terrestrial and aquatic plants. Our results from the central Tibetan Plateau shows such potential, because C4 herbs and submerged macrophytes are clearly separated by  $C_{max}$ , as the former is grouped with other terrestrial herbs at C29 and C31, whilst the latter concentrates at C23 and C25 (Fig. 4a).

When the  $\delta^{13}C_{org}$  values are plotted against  $P_{aq}$ , submerged macrophytes can be clearly distinguished from C4 herbs (Fig. 4b). This is because the  $P_{aq}$  index for floating/submerged macrophytes tends to have a higher value between 0.45 and 1.00, whilst terrestrial vascular plants commonly have a value  $<0.45$  (Ficken et al., 2000; Mead et al., 2005). Hence, the combination of  $\delta^{13}C_{org}$  values and  $P_{aq}$  is useful tool for paleoenvironmental reconstructions from lake or wetland sediments. Similarly, several studies suggest a possible relationship between ACL and wet/dry climate conditions (e.g. Huang et al., 2000; Hughen et al., 2004; Ratnayake et al., 2006). Our results show that the ACL values of dryland and wetland herbs and shrubs overlap and range between 31 and 27 (Fig. 4c). ACL for trees and submerged macrophytes varies mostly between 28 and 24. To some extent, therefore, ACL can be used as an index to depict wet/dry habitat conditions, or it can be seen as an index for precipitation/evaporation ratios.

Previous studies suggest that epicuticular waxes of terrestrial plants usually have CPI values  $>5$  (Cranwell, 1984; Eglinton and Hamilton, 1967). However, other studies indicate the limitations of CPI values for differentiating vegetation types (Luo et al, 2012; Rao et al, 2009).

Our results show clear groupings that suggest potential of CPI for palaeoenvironmental reconstructions. CPI of tree samples is mostly >20 (Fig. 4d), whilst shrubs, herbs and submerged macrophytes between 5 and 15. Therefore, CPI may be a useful index to depict whether or not trees are present in the environment.

As discussed above, each of the  $\delta^{13}\text{C}_{\text{org}}$  value and *n*-alkane indices has its own utility in revealing sources of organic matter, and a combination between these two methods can be much more useful in palaeoenvironmental reconstructions. The potential of this approach is demonstrated when these methods are applied to a sediment core (CN01) which is collected also from the study area.

#### **4.2. $\delta^{13}\text{C}_{\text{org}}$ values and *n*-alkane indices from core CN01**

As suggested above, the sediment sequence from core CN01 can be divided into eight stages (Fig. 3). These stages represent periods of small changes in habitat conditions throughout the past 9,000 years. In other words, core CM01 provides an excellent opportunity for testing the usefulness of bulk and compound specific organic carbon isotopes and *n*-alkanes in assessing the relative contributions of organic sources between terrestrial vascular plants and aquatic macrophytes in the alpine meadow sediment sequence. The  $\delta^{13}\text{C}_{\text{org}}$  values and *n*-alkane indices from core CN01 show some small fluctuations between stages, suggesting minor changes in the habitat conditions.

Stage I was under fluvial conditions as the coarse sediment implies. The TOC is very low,



and thus its organic carbon result is less reliable. Nevertheless, the bulk  $\delta^{13}\text{C}_{\text{org}}$  values within this stage are relatively more enriched, suggesting an input of aquatic organic matter rather than C4 herbs because of the low  $C_{\text{max}}$  and high  $P_{\text{aq}}$  values (Fig. 3c, d, e). From Stage I to Stage II saw a change from sandy sediment to organic rich silt and clay, with TOC increased to around 40%, suggesting the establishment of a wetland habitat. This development is confirmed by the pollen data (e.g. Cheung et al., 2014), which indicate a change of vegetation from a Poaceae-Cyperaceae-Artemisia community to a Cyperaceae-dominated community. A significant increase in wetness of the site is also indicated by the PCA axis 1 of the pollen data (Fig. 3h).

Above Stage II, the sedimentation rate increased, and the bulk  $\delta^{13}\text{C}_{\text{org}}$  varies narrowly between -24.8‰ and -27.8‰ (Fig. 3c). These values are very close to that of the C3 terrestrial plant end member (Table 1), indicating C3 terrestrial plant as the dominant source of organic matter. In Stages III, V and VII, the bulk  $\delta^{13}\text{C}_{\text{org}}$  are slightly enriched. As the  $P_{\text{aq}}$  values in these Stages are all  $>0.45$  (Fig. 3e), indicating an input of organic matter from submerged macrophytes rather than C4 herbs. Comparatively, the bulk  $\delta^{13}\text{C}_{\text{org}}$  in Stages IV, VI and VIII are more depleted, which coincides with lower  $P_{\text{aq}}$  values, implying a reduction of organic input from submerged macrophytes. The changes in both the bulk  $\delta^{13}\text{C}_{\text{org}}$  and  $P_{\text{aq}}$  values may suggest that despite the fact that the wetland was largely covered by C3 wetland herbs such as sedges, a relatively larger open water area within the wetland in Stages III, V

and VII, during which slightly more submerged macrophytes were present. In Stages IV, VI, and VIII, the area of open water within the wetland may have been smaller, thus proportionally smaller amount of submerged macrophytes was present.

The above interpretation is supported by further evidence. Firstly, the dominant wetland herb community is made of Cyperaceae, which accounts for >60% of the total land pollen during Stage II through to Stage VII (e.g. Cheung et al., 2014). These Cyperaceae are predominantly C3 as the mostly depleted bulk and compound specific  $\delta^{13}\text{C}_{\text{org}}$  values (Table 5) suggest. A field survey also reported that C4 herbs are sparse in the central Tibetan Plateau (Wang, 2003). Secondly, the  $\text{CPI}_{23-31}$  index is below 20 for all the stages (Fig. 3g), indicating very few trees were present around the wetland. In fact, tree pollen is <3% of total land pollen throughout the core (Cheung et al., 2014). Finally, the occasional increase of organic input from submerged macrophytes possibly due to an increase in the size of open water area or in the productivity of submerged macrophytes within the wetland is supported by the  $\text{ACL}_{23-31}$  index. This index shows weaker evaporation during Stages III, V and VII and stronger evaporation in Stages IV, VI and VIII (Fig. 3f). Despite the usefulness of the combined  $\delta^{13}\text{C}_{\text{org}}$  and *n*-alkanes methods, a note of caution must be mentioned. At present, the *n*-alkane indices from sediments should be used in palaeoenvironmental reconstructions qualitatively rather than quantitatively, because there are still uncertainties surrounding *n*-alkanes production from various types of plant, their transportation and deposition, as well as

post-depositional processes. In this respect, the higher or lower than 0.45 values of  $P_{aq}$  in the sediment core should only be interpreted as an indication of an increase or reduction in aquatic plant matter input.

#### **4.3. Comparison of regional records**

The reconstructed environmental history from core CN01 shows some similarity and differences with palaeo-environmental records from both the Asian monsoon dominated region (i.e. along the eastern edge of Tibetan Plateau and areas east and southeast of the Plateau) and the westerlies dominated region (i.e., northwestern Tibetan Plateau and areas north and northwest of the Plateau). Firstly, in the Asian monsoon dominated region, palaeo-records indicate generally a stable climate in the Holocene. For instance, peat accumulation has continued throughout the Holocene at Zoige-Hongyuan peatland (e.g. Yan et al., 1999; Hong et al., 2003; Zhao et al., 2011). The total organic carbon from a core from the Zoige Basin shows a similar trend as the core CN01, i.e. high and stable TOC during the middle Holocene and large fluctuations (e.g. Zhao et al., 2011) or a significant decline (e.g. Zheng et al., 2007) in TOC during the late Holocene (Fig. 5a, d). This trend implies a relatively stable precipitation throughout the Holocene till the last 2000 years, which seems follow largely the precipitation history recorded at the Dongge Cave (e.g. Wang et al., 2005) (Fig. 5g). However, a major difference between central Tibet and the Asian monsoon dominated region appears in the onset time of peat accumulation, about 2000 years earlier at

Zoige-Hongyuan peatland than that in central Tibet (Fig. 5a, d, g). The late start in peat accumulation in central Tibet may be caused by the strong influence of the Westerlies which had led to a low water level (even dry out, e.g. Chen et al., 2008) in many lakes in the Westerlies dominated region before 8000 cal. yrs BP of the Holocene. In other words, the coarse basal sediment in core CN01 is a result of the dry climate influenced by the strong Westerlies in the early Holocene, during which the Asian monsoon dominated region had already received strong supply of moisture from the summer monsoon.

Secondly, the multiple changes in  $\delta^{13}\text{C}_{\text{org}}$  values and *n*-alkanes indices swinging between terrestrial dominated and aquatic dominated end members throughout the Holocene (Fig. 5b, c) are also observed from a peat core from Hongyuan-Zoige peatland (e.g. Hong et al., 2003; Zheng et al., 2007) (Fig. 5e, f). Such fluctuations in  $\delta^{13}\text{C}_{\text{org}}$  values and *n*-alkanes indices in both central Tibet and Hongyuan-Zoige peatland suggest small-scale changes in the strength of precipitation and evaporation to these study sites. The short-duration precipitation/evaporation changes may reflect the fact that: although the precipitation history of the study area was controlled largely by the Asian monsoon precipitation as the TOC records indicate, the variability of North Atlantic climate was also transmitted to the study area by the Westerlies resulting in these multiple small-scale dry events recorded in central Tibet and the monsoon dominated region. It is noted that these short-term dry events are also reported from the Dongge Cave (e.g. Wang et al., 2005).

## 5. Conclusions

This study examined both the bulk and compound specific organic carbon isotopes and lipid *n*-alkanes from plants and a sediment core from the central Tibetan Plateau. Both the organic carbon isotopes and *n*-alkanes indices from the modern plants indicate some distinctive differences between terrestrial plants and aquatic plants. Their organic carbon isotope and *n*-alkanes signatures, therefore, can assist with palaeoenvironmental reconstructions. Our results suggest a combination of these indices can help expand the potential of these methods and greatly improve palaeoenvironmental studies.

The combined studies of organic carbon isotopic ratios and the *n*-alkanes indices in the sediment core provide details of the environmental history for the Dangxiong wetland, a representative of the Holocene climatic history for central Tibet. This wetland recorded a change from fluvial conditions to a wetland habitat around 8000 years ago, which was followed by a stable wetland environment throughout the middle-late Holocene with some significant changes during the last 2000 years. Our combined organic carbon isotopes and *n*-alkanes methods provide further details of the environmental history for the past 8000 year period, during which there have been small-scale changes in the wetland in the form of expansion and contraction of open water area or in the productivity of submerged macrophytes/aquatic plants within the wetland ecosystem. These changes may be caused by

external influence such as global climate change or internal processes in organic matter production and deposition.

### **Acknowledgements**

This study is funded by the HKSAR Research Grant Council (HKU700109P). The organic carbon isotope measurements are supported by the Faculty of Science Central Facility of HKU and by the Special Equipment Grant (SEG-HKU01) from the University Grants Committee of HKSAR. The authors are grateful to the constructive comments from the three anonymous reviewers, whose suggestions have help greatly improve the paper.

### **References**

- Aichner, B., Herzschuh, U., Wikes, H., 2010. Influence of aquatic macrophytes on the stable carbon isotopic signatures of sedimentary organic matter in lakes on the Tibetan Plateau. *Organic Geochemistry* 41, 706-718.
- Chen, F., Yu, Z., Yang, M., Ito, E., Wang, S., Madsen, D.B., Huang, X., Zhao, Y., Sato, T., Birks, H.J.B., Boomer, I., Chen, J., An, C., Wünnemann, B. 2008. Holocene moisture evolution in arid central Asia and its out-of-phase relationship with Asian monsoon history. *Quaternary Science Reviews*, 27, 351-364.
- Cheung, M.C., Zong, Y., Zheng, Z., Huang, K., Aitchison, J.C., 2014. A stable mid-late Holocene monsoon climate of the central Tibetan Plateau indicated by a pollen record. *Quaternary International* 333, 40-48.
- Cranwell, P.A., 1984. Lipid geochemistry of sediments from Upton Broad, a small productive lake.

Organic Geochemistry 7, 25-37.

Cranwell, P.A., Eglinton, G., Robinson, N., 1987. Lipids of aquatic organisms as potential contributors to lacustrine sediments – II. Organic Geochemistry 11, 513-527.

Eglinton, G., Hamilton, R.J., 1967. Leaf epicuticular waxes. Science 156, 1332-1335.

Ficken, K.J., Li, B., Swain, D.L., Eglinton, G., 2000. An n-alkane proxy for the sedimentary input of submerged/floating freshwater aquatic macrophytes. Organic Geochemistry 31, 745-749.

Hong, Y.T., Hong, B., Lin, Q.H., Zhu, Y.X., Shibata, Y., Hirota, M., Uchida, M., Leng, X.T., Jiang, H.B., Xu, H., Wang, H., Yi, L. 2003. Correlation between Indian Ocean summer monsoon and North Atlantic climate during the Holocene. Earth and Planetary Science Letters 211, 371-380.

Huang, Y., Dupont, L., Sarnthein, M., Hayes, J.M., Eglinton, G., 2000. Mapping of C4 plant input from North West Africa into North East Atlantic sediments. Geochimica et Cosmochimica Acta, 64(20), 3505-3513.

Huang, Y., Street-Perrott, F.A., Metcalfe, S.E., Brenner, M., Moreland, M., Freeman, K.H., 2001. Climate change as the dominant control on glacial-interglacial variations in C3 and C4 plant abundance. Science, 293(5535), 1647-1651.

Hughen, K.A., Eglinton, T.I., Xu, L., Makou, M., 2004. Abrupt tropical vegetation response to rapid climate changes. Science, 304(5679), 1955-1959

Kohn, M., 2010. Carbon isotope compositions of terrestrial C3 plants as indicators of (paleo) ecology and (paleo) climate. National Academy of Sciences, 107(46), 19691-19695.

Körner, Ch., Farquhar, G.D., Roksandic, Z., 1988. A global survey of carbon isotope discrimination in plants from high altitude. Oecologia, 74(4), 623-632.

Lamb, A. L., Leng, M.J., Umer Mohammed, M. Lamb, H.F., 2004. Holocene climate and vegetation change in the Main Ethiopian Rift Valley, inferred from the composition (C/N and  $\delta^{13}C$ ) of lacustrine organic matter. Quaternary Science Reviews, 23(7-8), 881-891.

Lin, X., Zhu, L., Wang, Y., Wang, J., Xie, M., Ju, J., Mausbacher, R., Schwalb, A., 2008. Environmental changes reflected by n-alkanes of lake core in Nam Co on the Tibetan Plateau since 8.4 ka BP.

- Chinese Science Bulletin 53, 3051-3057.
- Luo P., Peng P., Lu H., Zhou Z., Xu W., 2012. Latitudinal variations of CPI values of long-chain n-alkanes in surface soils: Evidence for CPI as a proxy of aridity. *SCIENCE CHINA Earth Sciences*, 55(7), 1134-1146.
- Mead, R., Xu, Y., Chong, J., Jaffé, R., 2005. Sediment and soil organic matter source assessment as revealed by the molecular distribution and carbon isotopic composition of n-alkanes. *Organic Geochemistry* 36, 363-370.
- Ménot, G., Burns, S.J., 2001. Carbon isotopes in ombrogenic peat bog plants as climatic indicators: calibration from an altitudinal transect in Switzerland. *Organic Geochemistry*, 32(2), 233-245.
- Meyers, P.A., Ishwatari, R., 1993. Lacustrine organic geochemistry – an overview of indicators of organic matter sources and diagenesis in lake sediments. *Organic Geochemistry* 20, 867-900.
- Meyers, P.A. 1994. Preservation of elemental and isotopic source identification of sedimentary organic matter. *Chemical Geology*, 114, 289-302.
- Mügler, I., Gleixner, G., Günther, F., Mäusbacher, R., Daut, G., Schütt, B., Berking, J., Schwalb, A., Schwark, L., Xu, B., Yao, T., Zhu, L., Yi, C., 2010. A multi-proxy approach to reconstruct hydrological changes and Holocene climate development of Nam Co, Central Tibet. *Journal of Paleolimnology* 43, 625-648.
- Rao, Z., Zhu, Z., Wang, S., Jia, G., Qiang, M., Wu, Y., 2009. CPI values of terrestrial higher plant-derived long-chain n-alkanes: a potential paleoclimatic proxy. *Frontiers of Earth Science in China*, 3(3), 266-272.
- Ratnayake, N.P., Suzuki, N., Okada, M., Takagi, M., 2006. The variations of stable carbon isotope ratio of land plant-derived n-alkanes in deep-sea sediments from the Bering Sea and the North Pacific Ocean during the last 250,000 years. *Chemical Geology*, 228(4), 197-208.
- Rieley, G., Coilier, R.J., Jones, D.M., Eglinton, G., Eakin, P.A., Fallick, A.E., 1991. Sources of Sedimentary Lipids Deduced from Stable Carbon Isotope. *Nature* 325, 425-427.
- Sachse, D., Radke, J., Gleixner, G., 2006.  $\delta D$  values of individual n-alkanes from terrestrial plants



- along a climatic gradient - Implications for the sedimentary biomarker record. *Organic Geochemistry*, 37, 469-483.
- Sparks, J.P., Ehleringer, J. R., 1997. Leaf carbon isotope discrimination and nitrogen content for riparian trees along elevational transects. *Oecologia*, 109(3), 362-367.
- Stevenson, B.A., Kelly, E.F., McDonald, E.V., Busacca, A.J., 2005. The stable carbon isotope composition of soil organic carbon and pedogenic carbonates along a bioclimatic gradient in the Palouse region, Washington State, USA. *Geoderma*, 124(1-2), 37-47.
- Stuiver, M., Reimer, P.J., Braziunas, T.F., 1998. High-precision radiocarbon age calibration for terrestrial and marine samples. *Radiocarbon* 40, 1127-1151.
- Tieszen, L.L., Senyimba, M.M., Imbamba, S.K., Troughton, J.H., 1979. The distribution of C3 and C4 grasses and carbon isotope discrimination along an altitudinal and moisture gradient in Kenya. *Oecologia*, 37(3), 337-350.
- Wang, L., Lü, H., Wu, N., Chu, D., Han, J., Wu, Y., Wu, H., Gu, Z., 2004. Discovery of C4 species at high altitude in Qinghai-Tibetan Plateau. *Chinese Science Bulletin*, 49(13), 1392-1396.
- Wang, N., Zong, Y., Brodie, C.R., Zheng, Z., 2014. An examination of the fidelity of n-alkanes as a palaeoclimate proxy from sediments of Palaeolake Tianyang, South China. *Quaternary International* 333, 100-109.
- Wang, R. L., Scarpitta, S. C., Zhang, S. C., Zheng, M. P., 2002. Later Pleistocene/Holocene climate conditions of Qinghai-Xizhang Plateau (Tibet) based on carbon and oxygen stable isotopes of Zabuye Lake sediments. *Earth and Planetary Science Letters*, 203(1), 461-477.
- Wang, R.Z., 2003. C4 plants in the vegetation of Tibet, China, their natural occurrence and altitude distribution pattern. *Photosynthetica* 41, 21-26.
- Wang, Y., Cheng, H., Edwards, R.L., He, Y., Kong, X., An, Z., Wu, J., Kelly, M.J., Dykoski, C.A., Li, X. 2005. The Holocene Asian monsoon: links to solar changes and North Atlantic climate. *Science*, 308, 854-857.
- Yan, G, Wang, F.B., Shi, G.R., Li, S.F. 1999. Palynological and stable isotopic study of

palaeoenvironmental changes on the northeastern Tibetan plateau in the last 30,000 years. *Palaeogeography, Palaeoclimatology, Palaeoecology*, 153, 147-159.

Zhao, Y., Yu, Z., Zhao, W. 2011. Holocene vegetation and climate histories in the eastern Tibetan Plateau: controls by insolation-driven temperature or monsoon-derived precipitation changes? *Quaternary Science Reviews*, 30, 1173-1184.

Zheng, Y., Zhou, W, Meyers, P.A., Xie, S. 2007. Lipid biomarkers in the Zoige-Hongyuan peat deposit: indicators of Holocene climate changes in west China. *Organic Geochemistry*, 38, 1927-1940.

### Figure captions

Fig. 1. (a) A map indicating the study area in the central Tibetan Plateau, location of the sediment core and details of the landscape around the coring site CN01. (b) A cross-section showing the valley floor of the Dangqu River.

Fig. 2. Vegetation zones across the Tibet and sampling locations of modern plants in this study.

Fig. 3. (a) Lithostratigraphy and chronology of core CN01, (b) total organic carbon (TOC%), (c) bulk organic carbon isotope ratios ( $\delta^{13}\text{C}_{\text{org}}$ ), (d) carbon number of maximum alkane concentration ( $C_{\text{max}}$ ), (e) proportion of aquatic plant n-alkanes ( $P_{\text{aq}}$ ), (f) average carbon length ( $\text{ACL}_{(23-31)}$ ), (g) carbon preference index ( $\text{CPI}_{(23-31)}$ ), (h) principle component analysis axis 1 of the pollen data indicating wetter and dryer conditions, after Cheung et al. (2014). The palaeoenvironmental conditions are divided into eight stages.

Fig. 4. Bi-plots between *n*-alkanes indices and  $\delta^{13}\text{C}_{\text{org}}$  for trees, shrubs, herbs and submerged macrophytes.

Fig. 5. A comparison between the study site and records from the Asian monsoon dominated region. (a) Total organic content from core CN01, (b) organic carbon isotope ratios from core CN01, (c) the  $P_{aq}$  index from core CN01, (d) total organic carbon content from core ZB08-C1 of Zoige-Hongyuan peatland (after Zhao et al., 2011), (e) organic carbon isotop ratios from a core of Zoige-Hongyuan peatland (after Hong et al., 2003), (f)  $P_{aq}$  index from a core of Zoige-Hongyuan peatland (after Zheng et al., 2007), and (g) oxigen isotope ratios from Dongge Cave (after Wang et al., 2005).

Table 1. Bulk parameters of modern plant samples and their *n*-alkanes indices

Type	Species	Alt. (m)	Habitat	$\delta^{13}\text{C}_{\text{Org}}$	$\text{C}_{\text{max}}$	$\text{ACL}_{(23-31)}$	CPI	$P_{\text{aq}}$	ID	
Trees	Cupressaceae	3800	Riverside	-25.5	31	29.7	26.1	0.03	YZ6	
	Populus	3800	Riverside	-27.2	29	27.8	21.3	0.12	YZ3	
	Populus	4300	Garden	-26.7	27	27.3	13.8	0.21	TG04	
	Salix	3800	Sand dune	-25.2	27	26.7	32.4	0.26	YZ5	
	Salix	3800	Sand dune	-26.0	27	26.5	35.3	0.28	YZ10	
	Salix	4300	Garden	-26.7	25	25.5	44.3	0.73	TG03	
	Salix	4300	Garden	-25.6	25	25.4	31.5	0.75	TG02	
Shrubs	Rosaceae	3800	Dry slope	-24.9	31	29.4	14.8	0.09	YZ7	
	Caragana	3800	Dry slope	-23.6	29	27.6	2.9	0.26	YZ13	
	Caragana	3800	Dry slope	-25.0	29	28.1	11.9	0.14	YZ12	
	Caragana	4200	Dry slope	-24.6	29	27.8	7.9	0.25	CS8B	
C4 herbs	Cyperaceae	4200	Dry slope	-13.7	31	29.2	10.8	0.14	CS9B	
	Cyperaceae	4200	Dry slope	-13.4	31	29.2	6.1	0.17	CS14B	
	Cyperaceae	3800	Dry slope	-13.3	31	29.6	20.9	0.04	YZ22	
	Cyperaceae	4700	Dry slope	-15.3	29	29.4	7.8	0.07	ZN4B	
C3 herbs (dry)	Chenopodiaceae	5030	Dry slope	-27.1	31	28.8	3.3	0.17	EBC	
	Chenopodiaceae	3800	Dry slope	-26.8	31	29.9	8.1	0.01	YZ8	
	Plantago	3800	Sand dune	-26.7	31	30.0	6.4	0.03	YZ25	
	Poaceae	4200	Dry slope	-26.2	31	29.0	6.4	0.10	CS10B	
	Poaceae	6100	Dry slope	-25.7	31	29.5	8.5	0.07	HM8B	
	Cyperaceae	4650	Dry slope	-26.1	31	27.5	1.79	0.38	DW8B	
	Cyperaceae	4530	Lakeside	-26.1	31	28.9	7.7	0.18	NRP	
	Fabaceae	4700	Dry slope	-27.3	29	28.1	7.4	0.18	ZN1B	
C3 herbs (wet)	Cyperaceae	4200	Lakeside	-27.9	31	29.6	11.4	0.18	CS1B	
	Cyperaceae	3800	Riverside	-26.2	31	29.7	15.4	0.02	YZ20	
	Fabaceae	4500	Riverside	-27.6	31	30.4	14.2	0.02	LK04	
	Poaceae	5300	Riverside	-26.0	31	29.5	12.4	0.06	HM5B	
	Poaceae	4700	Riverside	-24.9	29	28.3	14.3	0.23	ZN13B	
	Poaceae	5700	Riverside	-25.9	29	29.5	16.0	0.06	HM6B	
	Asteraceae	4460	Lakeside	-26.1	29	28.4	14.2	0.16	YH02	
	Scrophulariaceae	4280	Lakeside	-24.9	29	28.6	6.6	0.10	DX02	
	Cyperaceae	4280	Lakeside	-26.7	29	28.0	5.1	0.19	DX01	
	Cyperaceae	4460	Lakeside	-25.6	29	28.9	11.2	0.03	YH01	
	Cyperaceae	4460	Lakeside	-26.2	29	28.4	12.2	0.12	YH2B	
	Submerged macrophytes*	Potamogeton	4610	Lake	-14.2	23	25.0	9.5	0.74	S-22P
		Potamogeton	2670	Lake	-16.6	25	26.4	11.0	0.54	S-26P

Potamogeton	4540	Lake	-8.8	23	25.1	9.4	0.74	Kou-Cha
Potamogeton	4100	Lake	-5.8	23	25.1	24.5	0.73	Donggi
Potamogeton	4700	Lake	-18.1	23	25.4	13.8	0.70	CTP-35
Potamogeton	4430	Lake	-15.4	25	25.6	6.3	0.70	LC-10
Potamogeton	4720	Lake	-7.9	23	25	13.2	0.78	CTP-20
Myriophyllum	4610	Lake	-9.7	23	24.3	3.3	0.89	S-22M
Myriophyllum	2670	Lake	-14.3	25	24.9	5.5	0.82	S-26M

---

\*After Aichner et al. (2010)

Table 2. Average  $\delta^{13}\text{C}$  value of odd carbon chain lengths for modern plant samples

No. samples per group	Bulk $\delta^{13}\text{C}$	C21	C23	C25	C27	C29	C31	Ave.
6 (trees)	-26.0		-32.2	-30.8	-30.0	-30.2	-30.2	-30.7
2 (shrubs)	-24.7		-28.9	-31.1	-32.2	-31.3	-31.7	-31.0
2 (C4 herbs)	-13.6	-19.2	-20.2	-25.6	-22.8	-24.1	-24.5	-22.7
6 (C3 dry-land herbs)	-26.7	-33.5	-32.8	-31.3	-33.1	-34.2	-33.1	-33.0
7 (C3 wetland herbs)	-26.4		-31.2	-32.2	-33.0	-32.9	-32.5	-32.4
9 (Submerged macrophytes)*	-12.7	-21.3	-19.2	-20.3	-22.7	-23.4	-25.6	-22.1

\*After Aichner et al. (2010)

Table 3. Lithostratigraphy of core CN01

Depth (m)	Descriptions
0.00 – 0.28	Fresh herbaceous plants in water
0.28 – 0.95	Very soft, saturated with water, greyish black humified organic clay with small amount of silt and random plant roots
0.95 – 5.20	Very soft, moist, black peat, with occasional plant roots
5.20 – 5.80	Soft, moist, brownish black fine sand with small pebbles at the base and gradual increase in organic matter (blackish peaty material) towards the top of the unit.

Table 4. Radiocarbon dates from core CN01

Depth (m)	Material	$^{14}\text{C}$ date (yr BP)	$\delta^{13}\text{C}$ (VPDB)	Calibrated age (yr BP) (2 sigma)	Median cal. age (yr BP)*	Laboratory code
1.10	Plant fragments	1790±30	-26.1	1620-1820	1720	Beta306051
1.59	Plant fragments	1930±30	-26.0	1820-1947	1880	Beta315961
2.39	Plant fragments	2580±30	-26.7	2718-2750	2730	Beta315962
3.72	Plant fragments	3840±30	-26.0	4151-4407	4280	Beta315963
4.17	Plant fragments	4220±30	-26.8	4630-4853	4740	Beta315964
4.71	Plant fragments	5200±30	-26.6	5909-5996	5950	Beta315965
5.36	Plant fragments	7380±40	-26.3	8084-8329	8190	Beta306052

\*Rounded to nearest decade.



Table 5. Average  $\delta^{13}\text{C}$  value for each zone of core CN01

No. samples per zone	$\delta^{13}\text{C}$	C21	C23	C25	C27	C29	C31	Ave.
6 from Zone VIII	-26.2	-31.4	-31.7	-33.8	-33.7	-33.0	-32.7	-31.8
6 from Zone VII	-25.4	-30.9	-31.6	-34.1	-33.2	-33.4	-33.2	-31.7
2 from Zone VI	-26.6	-30.2	-30.6	-31.2	-32.5	-31.2	-31.9	-30.6
7 from Zone V	-25.9	-31.0	-32.0	-34.8	-34.0	-34.1	-33.2	-32.2
3 from Zone IV	-26.9	-30.8	-31.6	-32.5	-33.4	-33.0	-32.8	-31.6
6 from Zone III	-25.9	-30.9	-31.9	-32.9	-32.8	-33.6	-32.6	-31.5
5 from Zone II	-26.6	-32.7	-33.5	-35.0	-35.9	-36.2	-35.1	-33.6
5 from Zone I	-25.9	-30.4	-31.3	-32.9	-33.9	-34.4	-32.1	-31.6

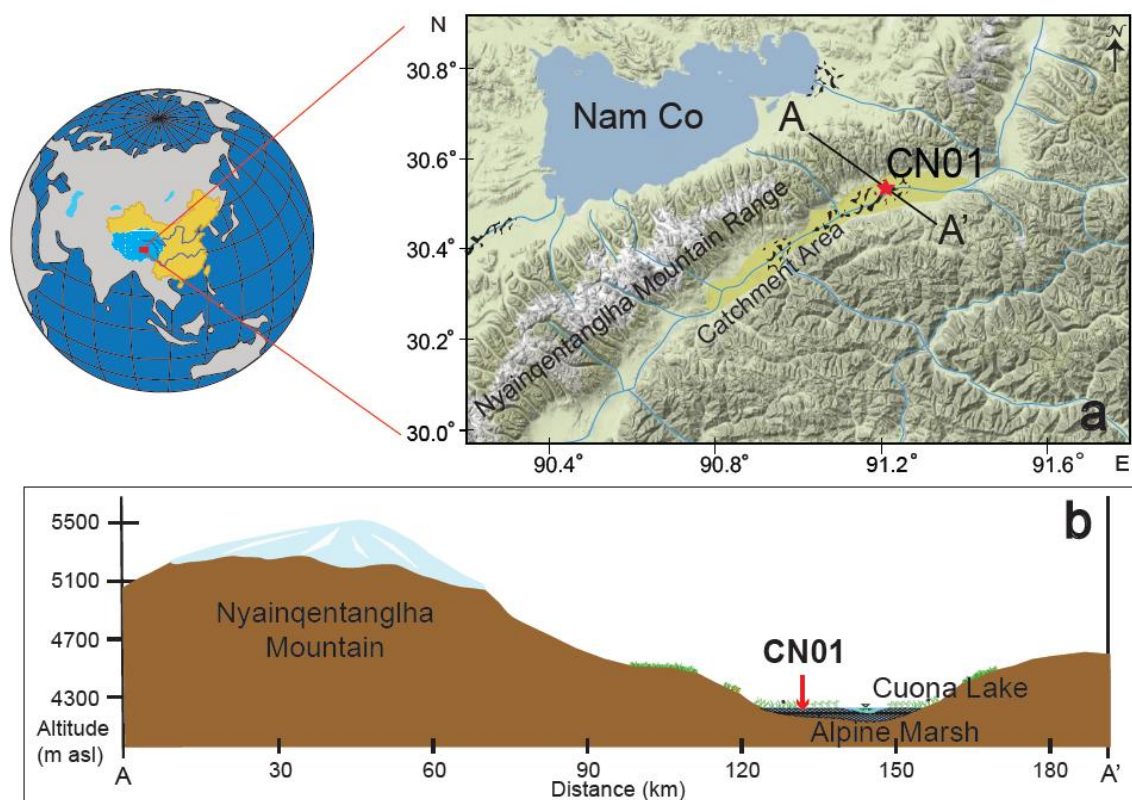


Figure 1

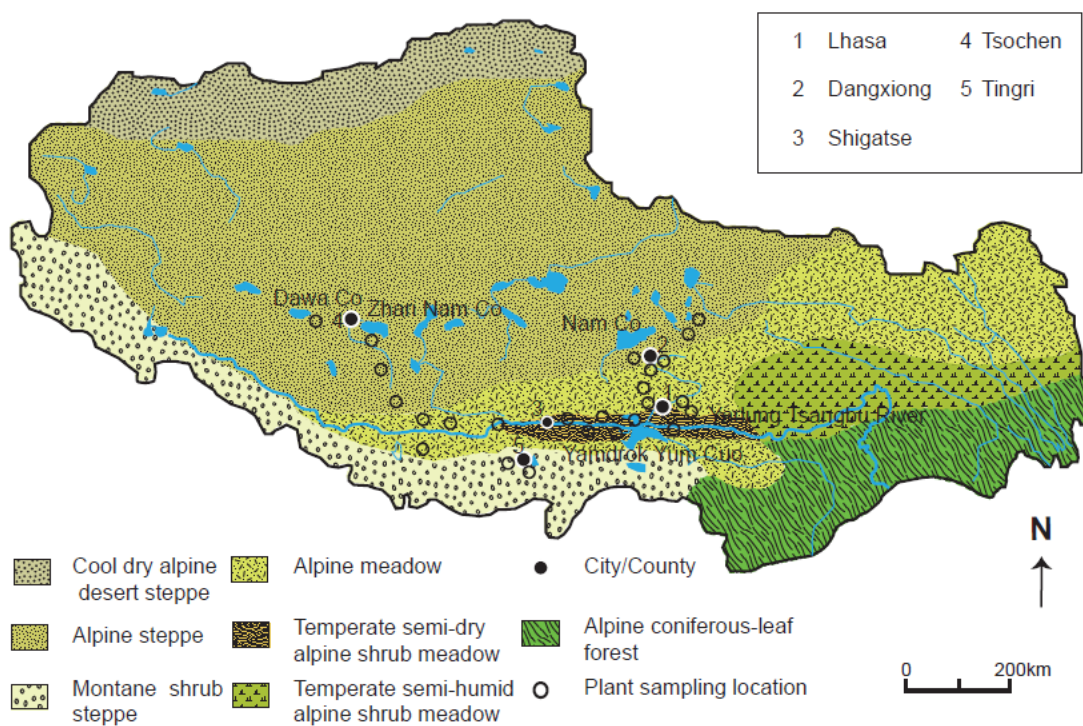


Figure 2

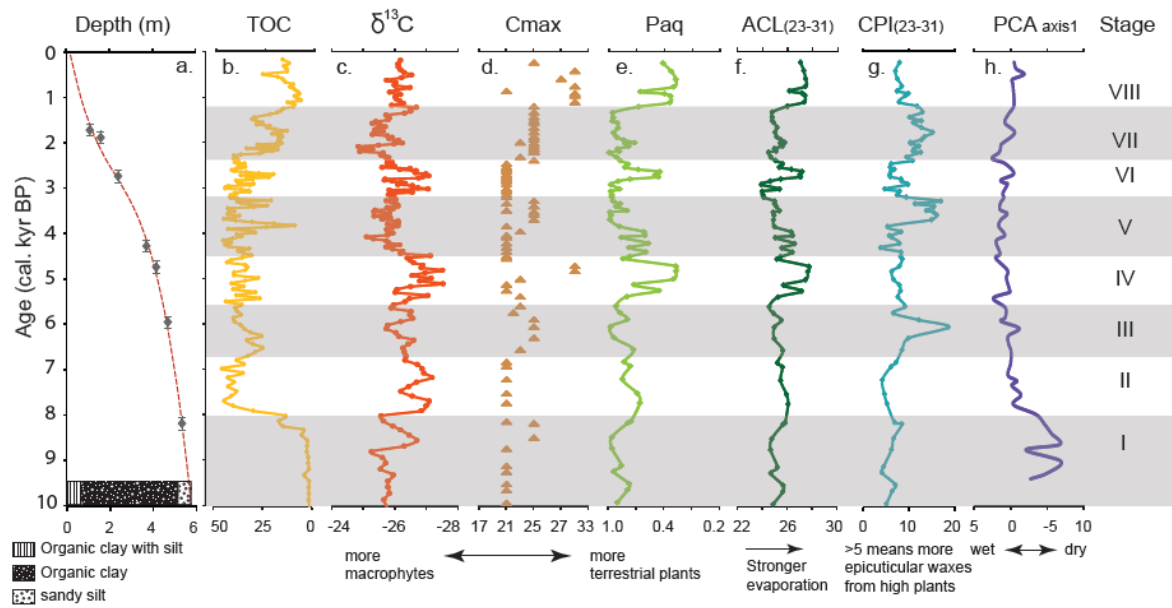


Figure 3

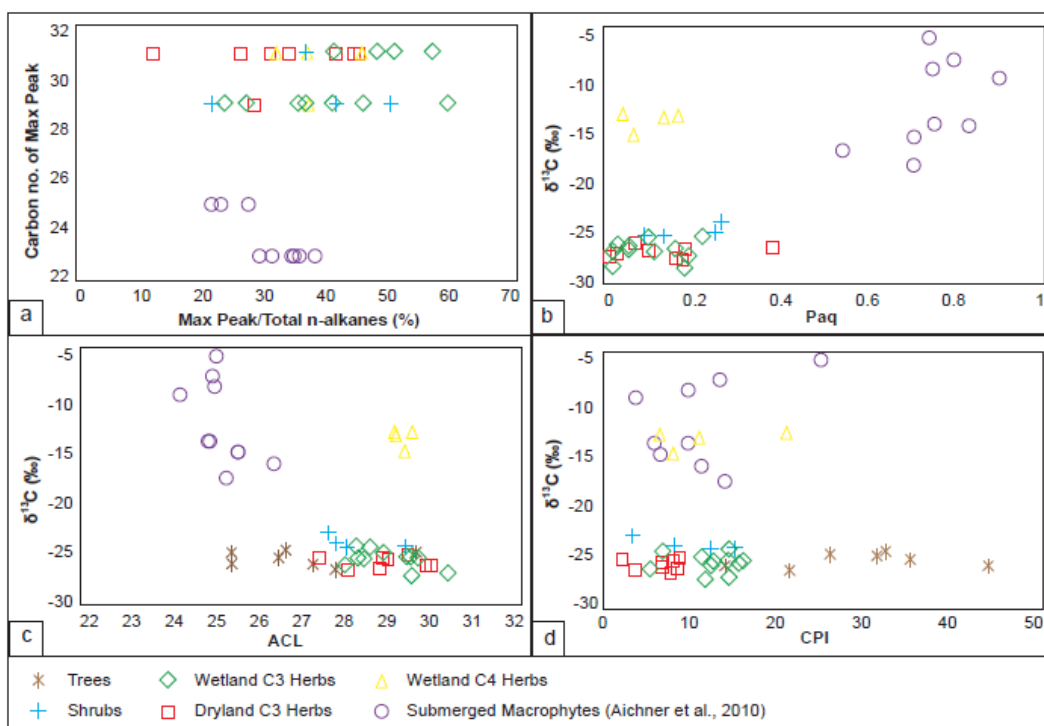


Figure 4

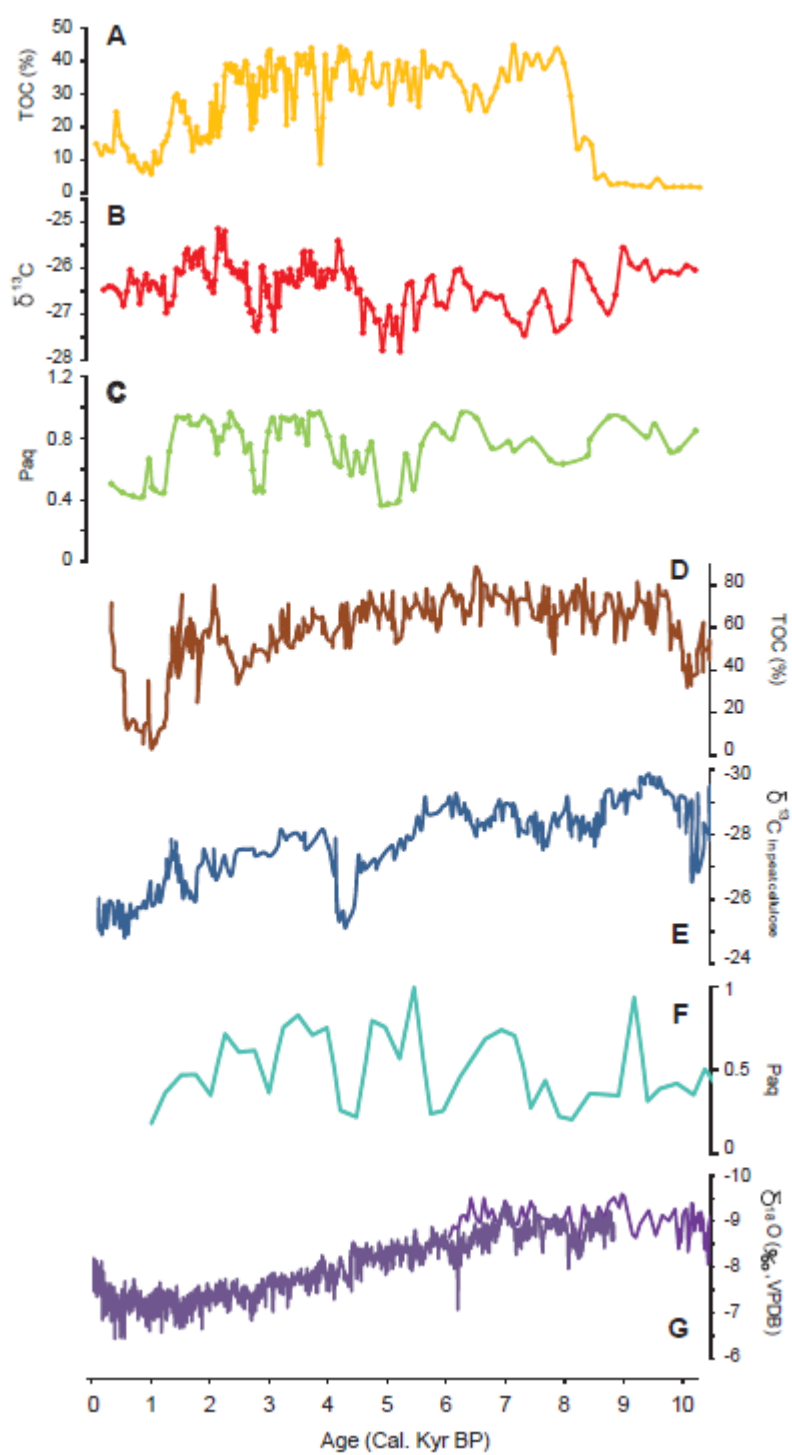


Figure 5

## Highlights:

- An examination of  $\delta^{13}\text{C}_{\text{org}}$  and lipid *n*-alkane indices from modern plants
- Combining  $\delta^{13}\text{C}_{\text{org}}$  and lipid *n*-alkanes for differentiating sources of organic matter
- Using *n*-alkane indices for palaeoenvironmental reconstructions
- Wetland condition changes under the stable climate of the mid-late Holocene